International Journal of Nanomedicine

Dovepress

open access to scientific and medical research

Open Access Full Text Article

ORIGINAL RESEARCH

Different Cell and Tissue Behavior of Micro-/Nano-Tubes and Micro-/Nano-Nets Topographies on Selective Laser Melting Titanium to Enhance Osseointegration

Xiaoran Yu[1,2,*]
Ruogu Xu[1,2,*]
Zhengchuan Zhang[1,2]
Qiming Jiang[1,2]
Yun Liu[1,2]
Xiaolin Yu[1,2]
Feilong Deng[1,2]

[1]Department of Oral Implantology, Hospital of Stomatology, Guanghua School of Stomatology, Sun Yat-Sen University, Guangzhou, Guangdong, 510055, People's Republic of China; [2]Guangdong Provincial Key Laboratory of Stomatology, Guangzhou, Guangdong, 510080, People's Republic of China

*These authors contributed equally to this work

Correspondence: Feilong Deng; Xiaolin Yu
Department of Oral Implantology, Hospital of Stomatology, Guanghua School of Stomatology, Sun Yat-Sen University, No. 56, Ling Yuan Xi Road, Guangzhou, 510055, People's Republic of China
Tel +86 20 83862537
Fax +86 20 83822807
Email dengfl@mail.sysu.edu.cn; yuxlin3@mail.sysu.edu.cn

Background and Purpose: Micro-/nano-tubes (TNTs) and micro-/nano-nets (TNNs) are the common and sensible choice in the first step of combined modifications of titanium surface for further functionalization in the purpose of extended indications and therapeutic effect. It is important to recognize the respective biologic reactions of these two substrates for guiding a biologically based first-step selection.

Materials and Methods: TNTs were produced by anodic oxidation and TNNs were formed by alkali-heat treatment. The original selective laser melting (SLM) titanium surface was set as control. Surface characterization was evaluated by scanning electron microscopy, surface roughness, and water contact angle measurements. Osteoclastogenesis and osteogenesis were measured. MC3T3-E1 cells and RAW 264.7 cells were used for *in vitro* assay in terms of adhesion, proliferation, and differentiation. *In vivo* assessments were taken on Beagle dogs with micro-CT and histological analysis.

Results: TNN and TNT groups performed decreased roughness and increased hydrophilicity compared with SLM group. For biological detections, the highest ALP activity and osteogenesis-related genes expression were observed in TNT group followed by TNN group ($P < 0.05$). Interestingly, when it comes to the osteoclastogenesis, TNNs displayed lowest TRAP activity and osteoclastogenesis-related genes expression and TNTs were lower than SLM but higher than TNNs ($P < 0.05$). BV/TV around implants was highest in TNT group after 4 weeks ($P < 0.05$). HE, ALP and TRAP staining showed that osteogenic and osteoclastic activity around TNTs were both higher than TNNs ($P < 0.05$).

Conclusion: TNNs and TNTs have dual advantages in promotion of osteogenesis and inhibition of osteoclastogenesis. Furthermore, TNNs showed better capability in inhibiting osteoclast activity while TNTs facilitated stronger osteogenesis. Our results implied that TNT substrates would take advantage in early application after implantation, while diseases with inappropriate osteoclast activity would prefer TNN substrates, which will guide a biologically based first-step selection on combined modification for different clinical purposes.

Keywords: multifunctional surface modifications, osteoclastogenesis, osteogenesis, custom-made titanium bone substitutes

Introduction

Nowadays, accuracy, flexibility, and speed as well as minimizing waste have become the emphases in manufacturing processes which promote the rapid development of three-dimensional (3D) printing. As a result, a wide range of material

types such as metals, ceramics and polymers have been successfully manufactured by 3D printing with desirable features.[1–4] Selective laser melting (SLM) is one of the prolific powder-bed based 3D printing technologies for metals. Through a layer-by-layer manufacturing method, SLM is capable of fabricating irregular and complex structures with high accuracy and shows huge potential in biomedical applications.[5,6]

Recently, researchers have reported custom-made titanium bone substitutes created by SLM with several advantages in manufacture.[7–10] Furthermore, for biomedical applications, the custom-made titanium bone substitutes should also possess special biological advantages for extended indications or therapeutic effect such as biomolecule or drug delivery. For example, Lee et al. reported a nanoparticle mediated PPARγ gene delivery on implants could be used as therapeutic dental implants for diabetic patients.[11] Zhang et al. reported that rhPDGF-BB loaded in nano-tube arrays could potentially be used in dental and orthopedic applications for osteoporotic patients.[12]

These biomedical applications rely on favorable osseointegration and the microenvironments induced by the titanium surfaces have played a significant role with various cells involved, such as mesenchymal stem cells, osteoblasts, osteoclasts and endothelial cells.[13–15] However, the original SLM titanium surface displayed poor cell behavior compared with the smooth surface.[16–18] One solution is surface modification to format bioactive surface topography for further functionalization. Various studies have focused on surface topography modifications for superior primary stability and early osseointegration.[19–21] Recent reports have declared that combining micro- and nano-topography could develop multiple advantages in promoting osteoconduction as well as increasing the adsorption of proteins and the migration of osteogenic cells.[22–24] Therefore, it is essential to understand the cellular mechanisms of different bioactive topographies in order to choose suitable individual surface modification for further functionalization targeted for specific patients.

Titanium dioxide nano-tubes (TNTs) topography is one of the widely noticed nano-topographies due to its excellent biocompatibility and enhanced bioactivity. Moreover, TNTs are well-controlled during manufacture since the production method, anodization, is a technology with simple operation and low cost.[25] Furthermore, TNTs exhibit a unique surface functionalization ability. Functionalized with biomolecules as well as loaded with therapeutic metal nano particles, antibiotics, or growth factors, TNTs show various special biomedical applications.[26] Cheng et al. reported the fabrication of strontium- and silver-loaded TNTs on titanium surfaces and demonstrated the enhanced antibacterial and osteogenesis properties.[27] A dual-controlled system, loading tetracycline grafted simvastatin-loaded polymeric micelles in TNTs, was constructed by Liu et al. and reported to improve local bone regeneration and osseointegration.[28]

On the other hand, titanium nano-nets (TNNs) topography is also extensively researched owing to the ECM-like structure and has demonstrated early and strong bone binding ability.[29–31] Alkali-heat treatment, involving immersion in sodium hydroxide solution and heating, is a common method to create TNNs topography with a sodium titanate layer.[32–34] At the same time, alkali-heat treatment is usually a pioneer step for depositing homogeneous bone-like apatite layer on surfaces.[35] This chemical-thermal treatment could activate bone-like apatite formation as well as keep space for cell migration, nutrients transport and matrix deposition.[36,37] Wang et al. reported that $SrTiO_3$ nanolayer coating on alkali-heat treated titanium possessed osteointegration promotion ability and long-term ion release capacity.[38]

As the nano-topographies with the property for further functionalization, the basic ability of TNTs and TNNs for osteogenesis has also been studied.[39,40] However, some limits still exist among previous investigations. It is well known that osseointegration build-up needs ongoing bone remodeling around interface, coupling osteoblasts and osteoclasts.[41] Most studies only focused on the behavior of osteoblasts in osseointegration but ignored the role of osteoclasts. On the other hand, there is still a lack of comparison between TNTs and TNNs on SLM titanium surfaces which could guide us to a suitable choice for individual surface modification on custom-made titanium bone substitute in order to treat specific patients.

Therefore, in this study, we aimed to compare the cell response on TNTs and TNNs of SLM titanium surface including osteogenesis and osteoclastogenesis behavior *in vitro*. Furthermore, the osseointegration of these two micro-nano topographies was also assessed *in vivo*. The results indicated the different cellular and tissue responses to micro-/nano-tubes and micro-/nano-nets topographies on SLM titanium, which would direct us to a reasonable first-step selection in multifunctional surface modification of custom-made titanium bone substitute.

Materials and Methods

Materials

Specimen Preparation

The SLM processing was reported in our previous study.[23] For *in vitro* cell assay, specimens were designed as titanium discs with 10 mm in diameter and 1 mm in thickness (Figure 1A). For *in vivo* animal study, specimens were designed as screw-shaped dental titanium implants (Figure 1B). The diameter is 4 mm and the length is 6 mm.

Surface Treatment

The original SLM titanium surface was set as the control group named SLM group after an ultrasonic processing in deionized water for 30 min.

The original SLM titanium experienced the physical-chemical treatment (sandblast-pickling) to reduce the roughness and improve the micro-topography. Then, both TNTs and TNNs were prepared on the surface of SLM titanium after sandblast-pickling.

TNTs were produced by anodic oxidation for 45 min with an applied voltage of 20 V. The electrolyte was ethylene glycol containing 3 vol% of deionized water and 0.3 wt% of NH_4F. This was the TNT group.

TNNs were produced by alkali heat treatment in 5 M NaOH solution at 80°C for 8 h and this group was named the TNN group.

Afterwards, all the specimens were sterilized by autoclave sterilizer. There were three groups termed SLM, TNT and TNN.

Surface Characterization

A field-emission scanning electron microscopy (FE-SEM, Hitachi, S-4800, Tokyo, Japan) was used to identify the surface topography. A 3D surface topography analyzer (BMT EXPERT, Lorsch, Germany) was employed to measure the surface roughness and an optical contact angle measuring device (Dataphysics, OCA40 Micro, Stuttgart, Germany) was used for investigating the surface wettability by the sessile-drop method.

In vitro Cell Behavior

Cell Culture Assay

MC3T3-E1 cells, the murine osteoblast-like cell line, were obtained from the Shanghai Cellular Institute of China Scientific Academy and used for evaluating osteogenesis activity. Cells were cultured in an α-MEM medium (Gibco, USA) containing 10% fetal bovine serum (FBS, Gibco, USA) and 1% penicillin-streptomycin (Gibco, USA).

As the murine preosteoclast cell line, RAW 264.7 cells used for evaluating osteoclastogenesis activity were obtained from Shanghai Zhong Qiao Xin Zhou Biotechnology Co, Ltd. Cells were maintained in DMEM medium with high glucose (Gibco, USA) supplemented with 10% FBS (Gibco, USA) and 1% penicillin-streptomycin (Gibco, USA). The osteoclastogenesis inducing medium containing 50 ng/mL receptor activator of nuclear factor kappa-B ligand (RANKL) and 20 ng/mL macrophage colony stimulating factor (m-CSF) were added.

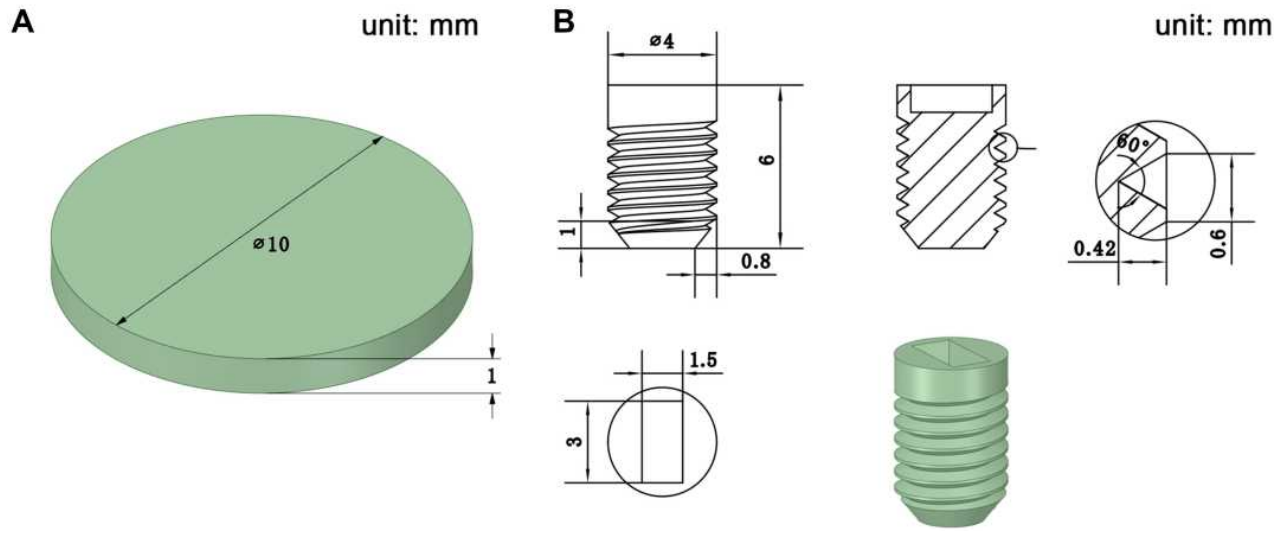

Figure 1 (**A**) Design sketch of specimens for *in vitro* cell assay; (**B**) Design sketch of specimens for *in vivo* animal study.

Table 1 Primers Used for Real-Time Polymerase Chain Reaction

Gene	Forward Primer Sequence (5′-3′)	Reverse Primer Sequence (5′-3′)
ALP	CCCACACTCAAGGGAGAGGT	GGAGGATTCCAGATACAGGCA
Runx2	CGGAGAGGTACCAGATGGGA	ATAACAGCGGAGGCATTTCG
OPG	TCAGCTCCTGTGTGACAAATGTG	TGTCCGTATAAGAGTGGTCAGGG
TRAP	GGCAGGTAAGATGGCTTTTGTG	TGACAACCCTCTGGATTTGGTT
c-Fos	CGGGTTTCAACGCCGACTA	TTGGCACTAGAGACGGACAGA
NFATc1	TGTGCAAGCCAAATTCCCT	CTTCTCTTCCGTTTCCCGTT
GAPDH	CTCCCACTCTTCCACCTTCG	TTGCTGTAGCCGTATTCATT

Abbreviation: GAPDH, glyceraldehyde-3-phosphate dehydrogenase.

Cell Adhesion

MC3T3-E1 and RAW 264.7 cells were seeded respectively onto each group at a density of 1×10^4 cells/mL in 48-well plates. At 24 h of culture, the specimens were taken out and fixed for 12 h in 2.5% glutaraldehyde solution. The specimens were then dehydrated in graded ethanol (50%, 75%, 90%, 95% and 100%) and dried. The adhesion morphology of cells was observed by SEM.

Cell Proliferation

The two types of cells were incubated same as above for 1, 4 and 7 days. A cell counting kit-8 assay (CCK-8, Dojindo, Kumamoto, Japan) was used for assessing cell proliferation. At each time point, the specimens were transferred to new 48-well plates and 500 mL of 10% CCK-8 fluid was added. After incubating for 2 h, optical absorbance (OD) at 450 nm was measured.

ALP Activity Assay of MC3T3-E1

Alkaline phosphatase (ALP) activity of MC3T3-E1 cells was measured at 7 and 14 days. Cells were lysed at 4°C for 30 min by 0.1% Triton X-100 (MP Biomedicals, Strasbourg, France) and supernatants were collected. The manufacturer's protocol (Jiancheng, Nanjing, China) was followed and absorbance at 520 nm was measured spectrophotometrically.

TRAP Activity Assay of RAW 264.7

RAW 264.7 cells were seeded for 7 and 14 days. After lysing, TRAP activity assay was made according to the manufacturer's instructions of a TRAP enzyme assay kit (Beyotime, Shanghai, China). An absorbance of 405 nm was measured.

Quantitative Real-Time PCR Analysis (qRT-PCR)

MC3T3-E1 and RAW 264.7 cells were respectively cultured on the specimen for 7 days. A TRIzol reagent (Invitrogen, Carlsbad, CA, USA) was used for isolating the total RNA based on the single-step method. The PrimeScriptRT MasterMix (TaKaRa, Kusatsu, Japan) was then used for synthesizing First-strand cDNA and qRT-PCR was carried out with SYBR Premix Ex Taq II (TaKaRa, Kusatsu, Japan) and specific oligonucleotide primers on a Light Cycler 480 (Roche, Basel, Switzerland). The osteogenesis marker genes (ALP, Runx2 and OPG) for MC3T3-E1 cells and the osteoclastogenesis marker genes (TRAP, c-Fos, NFATc1) for RAW 264.7 cells were measured. Table 1 showed the primer sequences and the mRNA levels for cells were normalized for GAPDH mRNA.

In vivo Animal Experiment

Survey

The animal study was approved by the Institution Animal Care and Use Committee (IACUC) of Sun Yat-Sen University (Approval No. SYSU-IACUC-2020-000244). During the animal experiment, the welfare and treatment of the laboratory animals were followed to "Animal management regulations of China" and "Guangdong experimental animal management regulations", which were published by State Scientific and Technological Commission of The People's Republic of China and People's Government of Guangdong Province, respectively. Five beagle dogs aged 1 year old were provided by Guangdong Frontier Biotechnology Co.

0.3 mg/kg pentobarbital sodium (pentobarbital sodium, Jilin, China) and 0.03 mg/kg xylazole (Sumianxin, Jilin, China) was used for anesthesia by intramuscular injection. Tooth extraction was taken from second premolar to first molar on the bilateral mandible and implant insertion was conducted after 3 months for bone healing. Three dogs were used for 4-week evaluation. Eight implants were inserted in bilateral mandible of each dog with different surface modification in a random order. Two dogs were used for 8-week evaluation, one was placed with 8 implants and only 4 implants were placed in unilateral mandible of the other (Figure 2). Gentamicin (Succhi

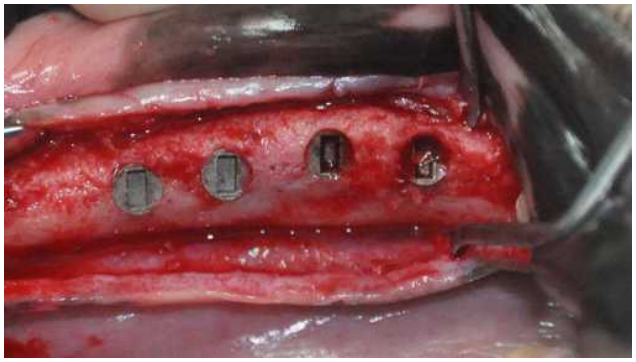

Figure 2 Surgical photo showing four implants placed in the unilateral alveolar ridge.

Shiqi, Guangdong, China) was injected 80,000 U each dog per day for 4 days after surgery. After 4 and 8 weeks, the dogs were sacrificed and specimens with implants and surrounding bone tissue were excised for further evaluation. Thus, 24 implants were obtained for 4-week evaluation and 12 were obtained for 8-week.

Micro-CT Evaluation

Micro-CT evaluation was conducted by a Micro-CT scanner (μCT50, Scanco Medical, Bassersdorf, Switzerland) for 1500 ms under 10 μm in resolution, 90 kV in voltage and 88 μA in current. Mimics® 19.0 was used for three-dimensional reconstruction. A cylinder-shaped tube (diameter: 5 mm, length: 6.5 mm) was placed on the same axle wire as well as the end overlapped with the shoulder of implant referring to the region of interest (ROI). A total 24 implants (12 for 4-week and 12 for 8-week, n = 4) were calculated for bone volumes (BV)/total volume (TV) of which BV referred to the bone tissues in ROI and TV referred to the volume of ROI.

Histological Analysis

After micro-CT evaluation, the specimens (n = 4) underwent hard tissue slicing. After dehydration and embedding, a EXAKT300CP microtome (EXAKT, Hamburg, Germany) was used for slicing the specimens into 200 μm thickness and EXAKT400S (EXAKT, Hamburg, Germany) was used for grinding sections into 25 μm. Methylene blue-acid fuchsin staining was performed and digital images were obtained at 25x magnification. BIC ratios were defined as the ratio of the bone length contact with implant to the implant length and calculated by Image J software (National Institutes of Health, MA, USA).

The remaining specimens excised after 4 weeks (n = 4) were decalcified. The implants were removed carefully and the specimens were made into paraffin section. HE staining, ALP staining and TRAP staining were performed and digital images at 40x magnification were obtained by a digital pathology scanner. The intensity of ALP was calculated and the TRAP positive cells were enumerated.

Statistical Analysis

Experiments *in vitro* were performed in triplicate. Data were expressed as the mean ± standard deviation (SD) and statistical analysis was conducted by one-way ANOVA with SPSS 23.0 (SPSS Inc., Chicago, USA). A P value of <0.05 was considered statistically significant.

Results

Surface Characterization

SEM images (Figure 3A) revealed that nano-nets with 100–120 nm in diameter and well-arranged nano-tubes with 70 nm in diameter were respectively established in TNN and TNT groups. The unmelted titanium particles and spheres were only seen in SLM group. 3D view of surface profiles in each group is shown in Figure 3B and the roughness was decreased to 3.41 μm (TNN group) and 7.09 μm (TNT group) of Ra value on average while roughness of original SLM titanium was approximately 12.58 μm (Table 2). The water contact angle of SLM group was 73.5 ± 3.25°, while those of TNN and TNT groups were 20 ± 1.66° and 23.5 ± 2.5° (Figure 3C), indicating more hydrophilicity.

In vitro Cell Behavior

Osteogenesis Assay

MC3T3-E1 cells (Figure 4A) were converged and obviously extended on each surface. On the surface of TNN and TNT group, MC3T3-E1 cells appeared flatter and more stretched, with more anchored lamellipodia and filopodia wrapping around the micro-/nano-nets and micro-/nano-tubes.

The cell proliferation was assessed by CCK-8, as shown in Figure 4B. At each time point, TNT group showed better proliferation than the other two groups ($P<0.05$). Besides, TNN group can also promoted more proliferation of MC3T3-E1 cells than SLM group ($P<0.05$).

ALP activity is the early marker of osteogenic differentiation and was measured at days 7 and 14. Results in Figure 4C showed the ALP activity of SLM, TNN and TNT gradually rose in sequence both at 7 and 14 days ($P<0.05$).

After culturing for 7 days, the osteogenic-related gene expression, including ALP, Runx2 and OPG, were upregulated in the groups of bioactive surfaces (Figure 4D–F).

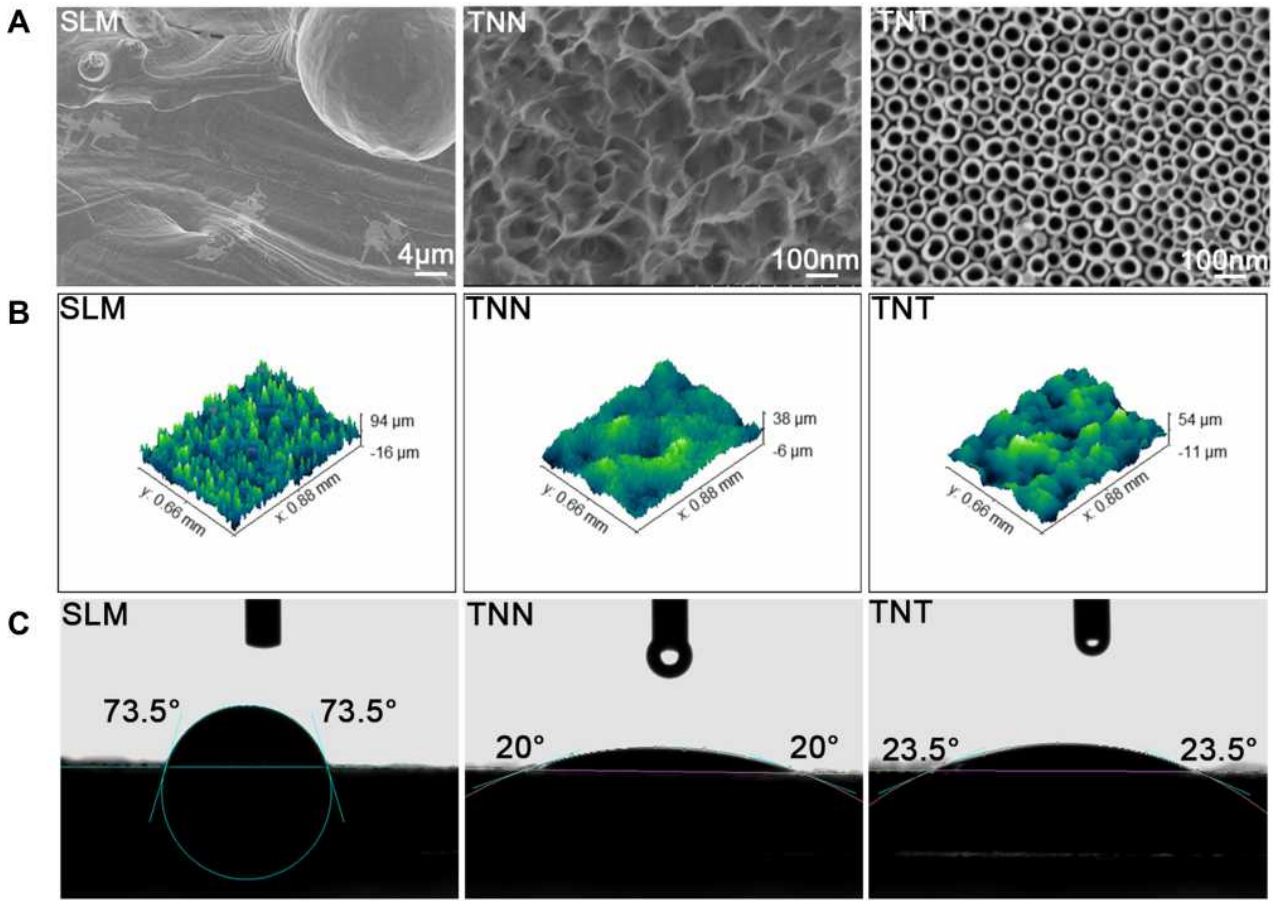

Figure 3 Surface characterization of the samples: (**A**) SEM images showing the surface topography of samples. SLM group (scale bar = 4 μm) showing waving surface with unmelted titanium particles and spheres, TNN group (scale bar = 100 nm) showing the nano-nets with 100–120 nm in diameter, TNT group (scale bar = 100 nm) showing the well-arranged nanotubes with 70 nm in diameter; (**B**) Surface roughness profiles of the samples; (**C**) Water contact angles of the samples.

Comparing among TNN and TNT groups, the micro-/nano-tubes seemed to show superior osteogenic differentiation ability than micro-/nano-nets.

Osteoclastogenesis Assay

The adhesion morphology of RAW 264.7 cells on bioactive surfaces had a great difference from that on original SLM surface (Figure 5A). On SLM surface, the cells were converged and extended. However, on the surfaces of TNN and TNT groups, the cells were adhered alone. Despite there being some lamellipodia wrapped onto the nano-structure, the cells still exhibited the ball shape, indicating a relative inhibition of function.

Table 2 Surface Roughness of the Samples

Group	SLM	TNN	TNT
Ra (μm)	12.58±1.07	4.31±0.57	7.09±0.72
Rq (μm)	16.07±0.88	5.39±0.71	9.50±0.54

Figure 5B showed the results of RAW 264.7 cells proliferation. Cellular proliferative activity was the lowest on the micro-/nano-nets surface ($P < 0.05$). TNTs surface could also suppress cell proliferation compared with the original SLM surface, although the inhibiting ability was lower than TNNs surface ($P < 0.05$).

When assessing the TRAP activity assay (Figure 5C), TNN-modified surfaces were significantly lower than TNT-modified surfaces ($P < 0.05$). Meanwhile, original SLM surface demonstrated the highest TRAP activity among the three groups ($P < 0.05$).

The gene expression of TRAP, c-Fos and NFATc1 was evaluated (Figure 5D–F), and the results were consistent with those above. TNN group displayed lowest expression of osteogenesis marker genes, and showed significant difference to TNT and SLM group ($P < 0.05$). In addition, TNT group also showed significantly lower expression than SLM group ($P < 0.05$).

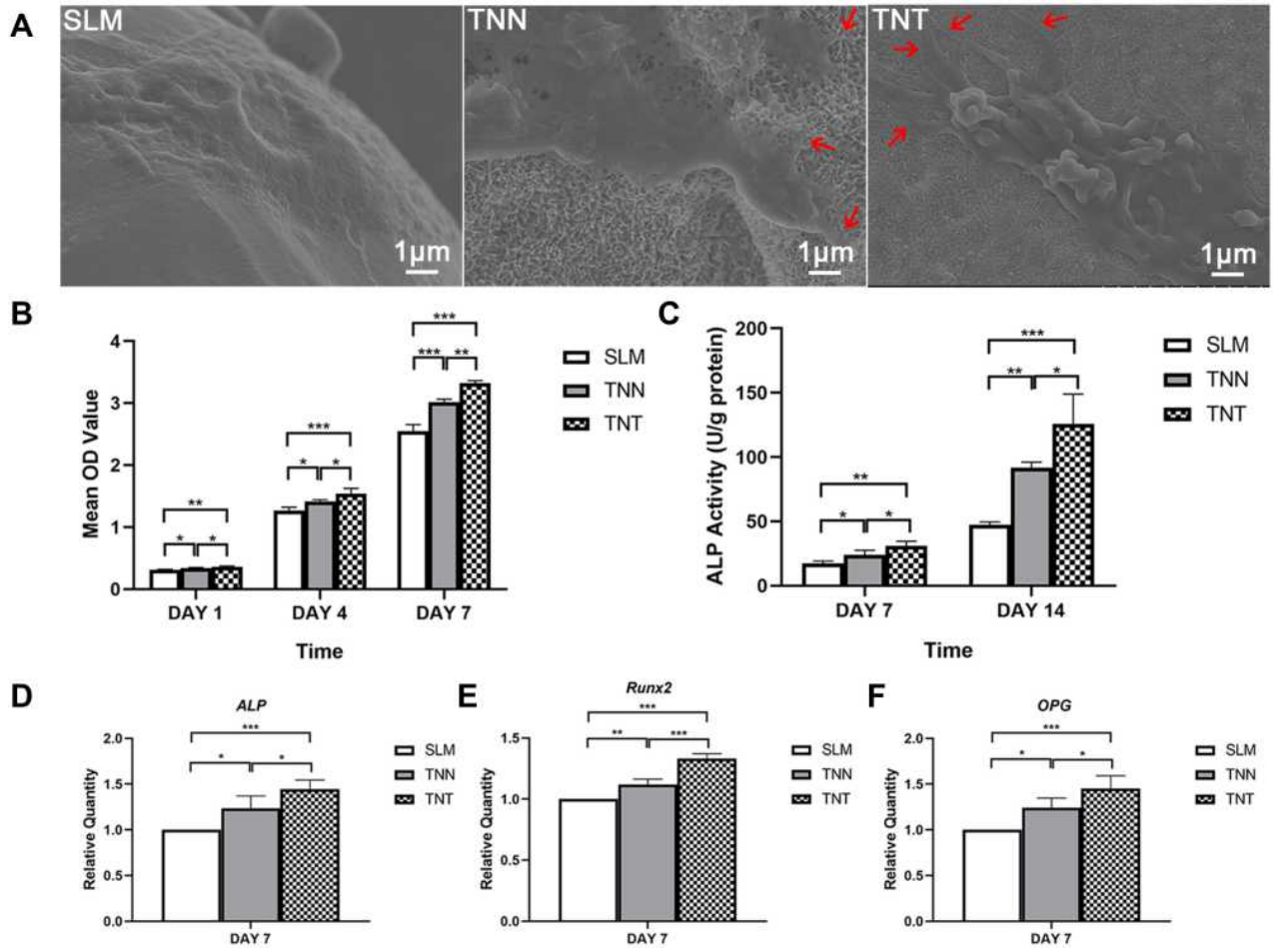

Figure 4 Results of osteogenesis assay *in vitro*: (**A**) Representative SEM images of MC3T3-E1 cells adhesion to the samples after 24 h (scale bar = 1 μm), more anchored lamellipodia and filopodia could be observed wrapping around the micro-/nano-nets and micro-/nano-tubes (red arrows); (**B**) Cell proliferation of MC3T3-E1 cells on the surfaces of the samples after 1, 4 and 7 days; (**C**) ALP activity assay of MC3T3-E1 cells on the surfaces of the samples after 7 and 14 days; (**D**–**F**) Gene expression relating to osteogenesis measured with quantitative real-time polymerase chain reaction after 7 days. *P <0.05, **P <0.01, ***P <0.001.

In vivo Animal Experiment

Micro-CT Evaluation

We used the mandible bone of beagle dogs as the animal model; thus, the environment around bone substitutes was in keeping with oral implantation. The three-dimensional reconstruction images are shown in Figure 6A. The groups with surface modification were higher BV/TV than SLM group as we expected (Figure 6B). Interestingly, BV/TV was statistically higher in TNT group than in TNN group after 4 weeks (P <0.05); while there was no evidence of difference after 8 weeks (P >0.05).

Histological Analysis

Figure 7A shows the methylene blue-acid fuchsin staining on undecalcified slices. SLM group owned the lowest BIC% at 4and 8 weeks (Figure 7B), representing the worst osseointegration (P <0.05). When comparing between TNN and TNT groups, results were consistent to the BV/TV ratio above in that TNT group showed larger BIC% at week 4 (P <0.05) but no statistical difference at week 8 (P >0.05).

The HE, ALP and TRAP staining were applied to detect the new bone formation, osteogenic and osteoclastic activity around the implants (Figure 8A). The red zone representing trabecular bone stained by H&E stain was thicker in TNN and TNT groups at week 4. Similarly, Figure 8B and C demonstrated that lowest osteogenic activity and highest osteoclastic activity were observed in SLM group (P <0.05). However, osteogenic and osteoclastic activity around TNTs were both higher than TNNs (P <0.05). This result may give the credit to the balance between osteogenesis and osteoclastogenesis, of course, implying accelerated osseointegration in early stage of TNT group as well as decreased bone resorption in later stage of TNN group.

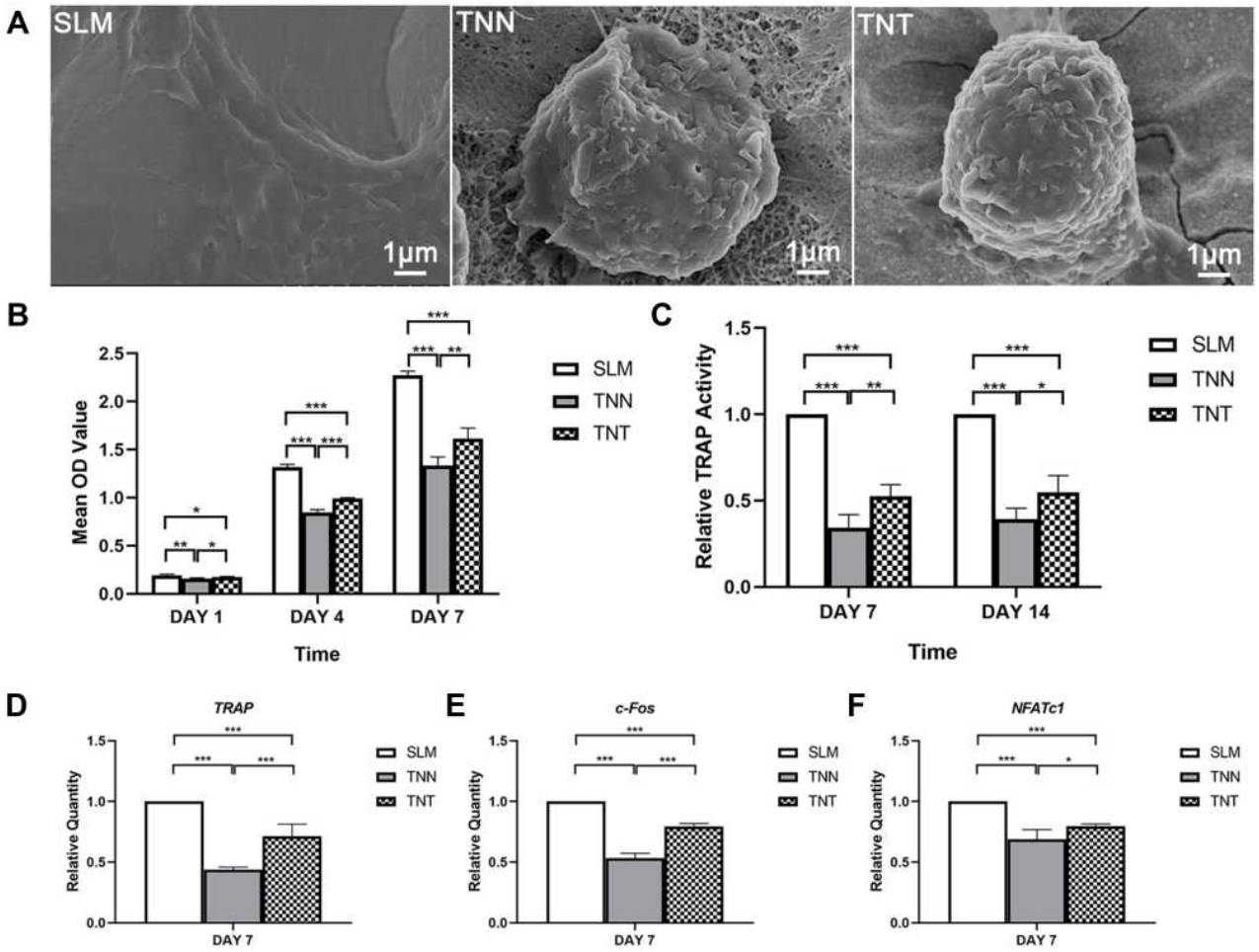

Figure 5 Results of osteoclastogenesis assay *in vitro*: (**A**) Representative SEM images of RAW 264.7 cells adhesion to the samples after 24 h (scale bar = 1 μm); (**B**) Cell proliferation of RAW 264.7 cells on the surfaces of the samples after 1, 4 and 7 days; (**C**) TRAP activity assay of RAW 264.7 cells on the surfaces of the samples after 7 and 14 days; (**D**–**F**) Gene expression relating to osteoclastogenesis measured with quantitative real-time polymerase chain reaction after 7 days. *P <0.05, **P <0.01, ***P <0.001.

Discussion

The multifunctional surface modification on titanium has been focused on individual-based treatment with customized implants for targeted patients. Numerous studies have successfully established bioactive surfaces loaded with metal particles, hydroxyapatite, drugs, as well as molecules. Pan et al. deposited zinc ions in TNTs, discovering the improvement of blood compatibility and the promotion of endothelialization for intravascular stents application.[42] Wu et al. fabricated the biomimetic titanium implant with mineralized extracellular matrix coated on the TNT surface, and confirmed the excellent osteogenic ability by increasing cell proliferation and calcium deposition.[43] Yang et al. covalently immobilized hyperbranched poly-L-lysine polymers onto TNN substrates to enhance antibacterial and osteointegration abilities at the same time.[44] Shen et al. reported that Mg/Zn-metal organic framework on TNN titanium possessed antibacterial and anti-inflammatory properties.[45] According to the above statement, TNN and TNT substrates are the common but wise choice for further functionalization with special nanostructure and excellent biocompatibility. Thus, it is important to recognize the different biologic reaction between TNN and TNT substrates, including the cellular behavior and osseointegration process, to remind us of a superior, biologically based selection playing a synergistic or complementary role for different clinical purposes. Therefore, SLM titanium substrates, mostly used for fabrication of customized implants, was selected to form TNN and TNT topographies in the present study. Meanwhile, the cellular behavior of osteoblast-like cells and preosteoclasts *in vitro* as well as overall

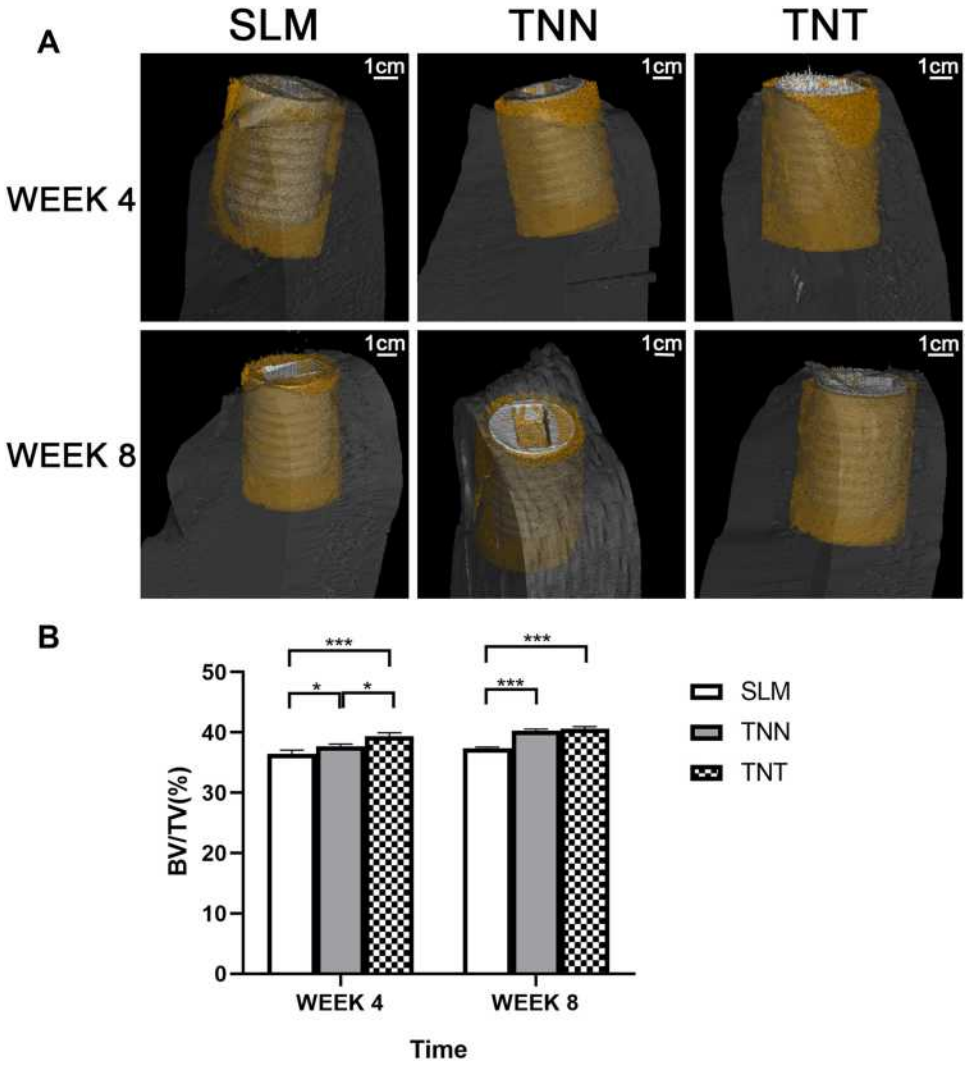

Figure 6 Micro-CT evaluation after 4 and 8 weeks: (**A**) Radiographs and 3D reconstruction of bone tissue around implants at 4 and 8 weeks (scale bar = 1 cm); (**B**) Statistical results of the bone volume/total volume (BV/TV). *P<0.05, ***P<0.001.

osseointegration *in vivo* could bring comprehensive knowledge of biological responses to TNNs and TNTs.

It is necessary to discuss the surface properties owing to the important role in regulating cell and tissue responses and further determining osseointegration, such as topography, roughness, and hydrophilicity.[46] Early research has concluded that the very rough SLM titanium surface needs bioactive treatments for better osteoblast differentiation.[47] Zhang et al. further indicated that roughness can mediate osteoclast-material interactions to determine the osteogenic differentiation and the process of osseointegration.[48] Before nano-modification, sandblasting-pickling was used in our study for decreased roughness, the same as our previous studies which would be appropriate for clinical application.[10,23] Our results showed the lower roughness on TNN group than TNT group, a possible interpretation of which could be the sodium titanate layer formed after alkali-heat treatment.[49] On the other hand, TNT and TNN groups were more hydrophilic, indicating better biocompatibility, than the SLM group in our study. However, some studies have reported the super-hydrophilic property with zero water contact angle in TNT titanium surface, which might be attributed to the inevitable contaminations of the substrate in the present study, for example, carbon and wrapping materials.[50] Moreover, the bioactivity of TNT titanium surface has been reported to be influenced by the diameter of TNTs. When it comes to the diameter of TNTs we selected in this study, we took into account the following two factors. First, Wang et al. reported that the optimal diameter of TNTs seemed to be around 70 nm with beneficial osteoconductivity.[51] Second, based on our purpose of this research, relatively large diameters would be more

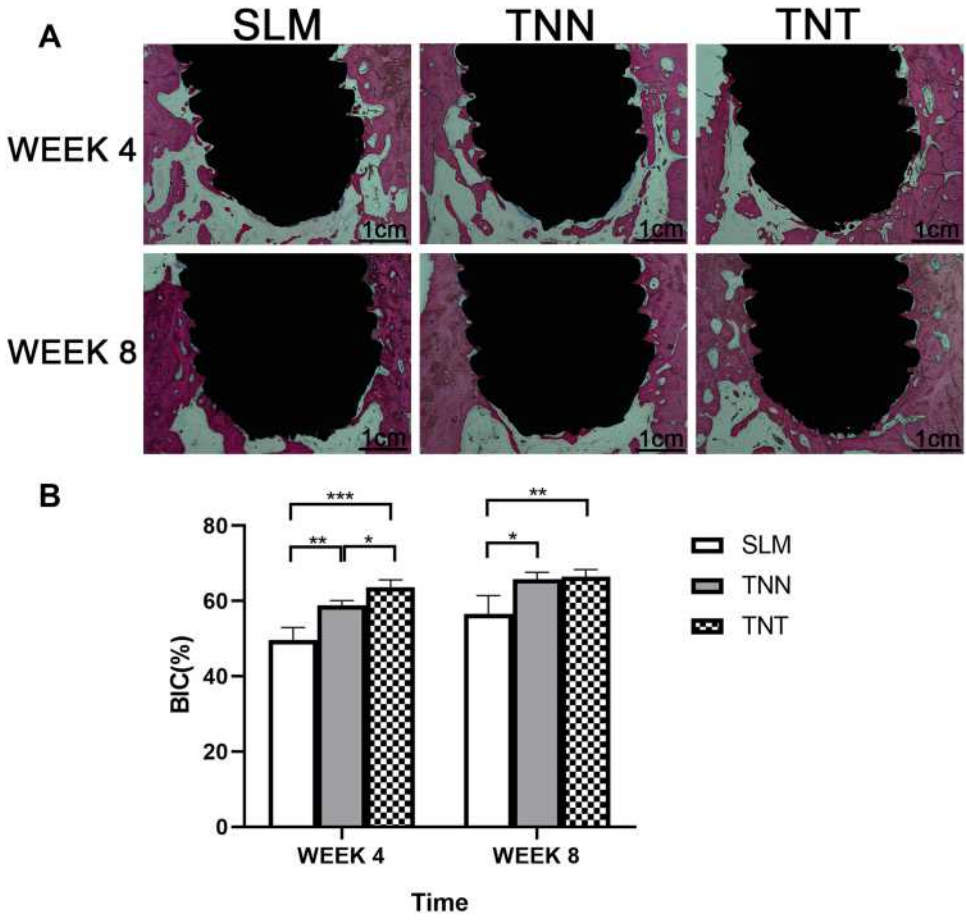

Figure 7 Histological analysis of undecalcified slices: (**A**) Methylene blue-acid fuchsin staining after 4 and 8 weeks (scale bar = 1 cm); (**B**) Statistical results of the percentage of bone-implant contact (BIC). *P <0.05, **P <0.01, ***P <0.001.

favored, allowing the deposition of more kinds of nanoparticles.

The groups with surface modification contributed to osteoblast-like cells adhesion and we inferred that nano-topography could enhance cells spreading by promoting the clustering of integrins.[19] Meanwhile, the extended adhesion area could promote the osteogenic activity agreed with our results. Among osteogenesis marker genes evaluated by qPCR, the transcription factor Runx2 plays an essential role in osteoblast differentiation which could induce osteocalcin, osteopontin and bone sialoprotein expression in non-osteoblastic cells.[52,53] OPG is also a mediator of bone metabolism leading to bone formation.[54] Together with CCK-8 and ALP assay, evidences showed the enhancement of osteogenic activity, consistent with the results of Wang et al. and Stan et al., comparing TNNs and TNTs with original surface in terms of osteogenesis, respectively.[38,55] Besides, our study also indicated stronger osteogenesis on TNT substrates than TNN substrates.

Few studies focus on the influence of surface modification on osteoclast differentiation, an essential and indispensable part of bone remodeling. Different from the adhesion morphology of osteoblast-like cells, preosteoclast adhered alone in ball shape on the modified surface, implying inhibited osteoclastogenesis. NFATc1, which could be induced and translocated by c-Fos, is a downstream target of NF-κB signaling, the critical pathway during osteoclast differentiation.[56–58] The expression of NFATc1 and c-Fos, together with the results of TRAP-related evaluation, informed us that the NF-κB pathways might also be regulated by TNN and TNT topographies so as to suppress the osteoclast differentiation. What is worth to note is that TNN could be more effective in terms of the inhibition of osteoclast differentiation according to the previously mentioned results. Furthermore, our previous study reported that TNNs could inhibit osteoclast differentiation through the MAPK signaling pathway.[59] Therefore, TNN substrates could play a stronger role in inhibiting osteoclastogenesis than TNT substrates.

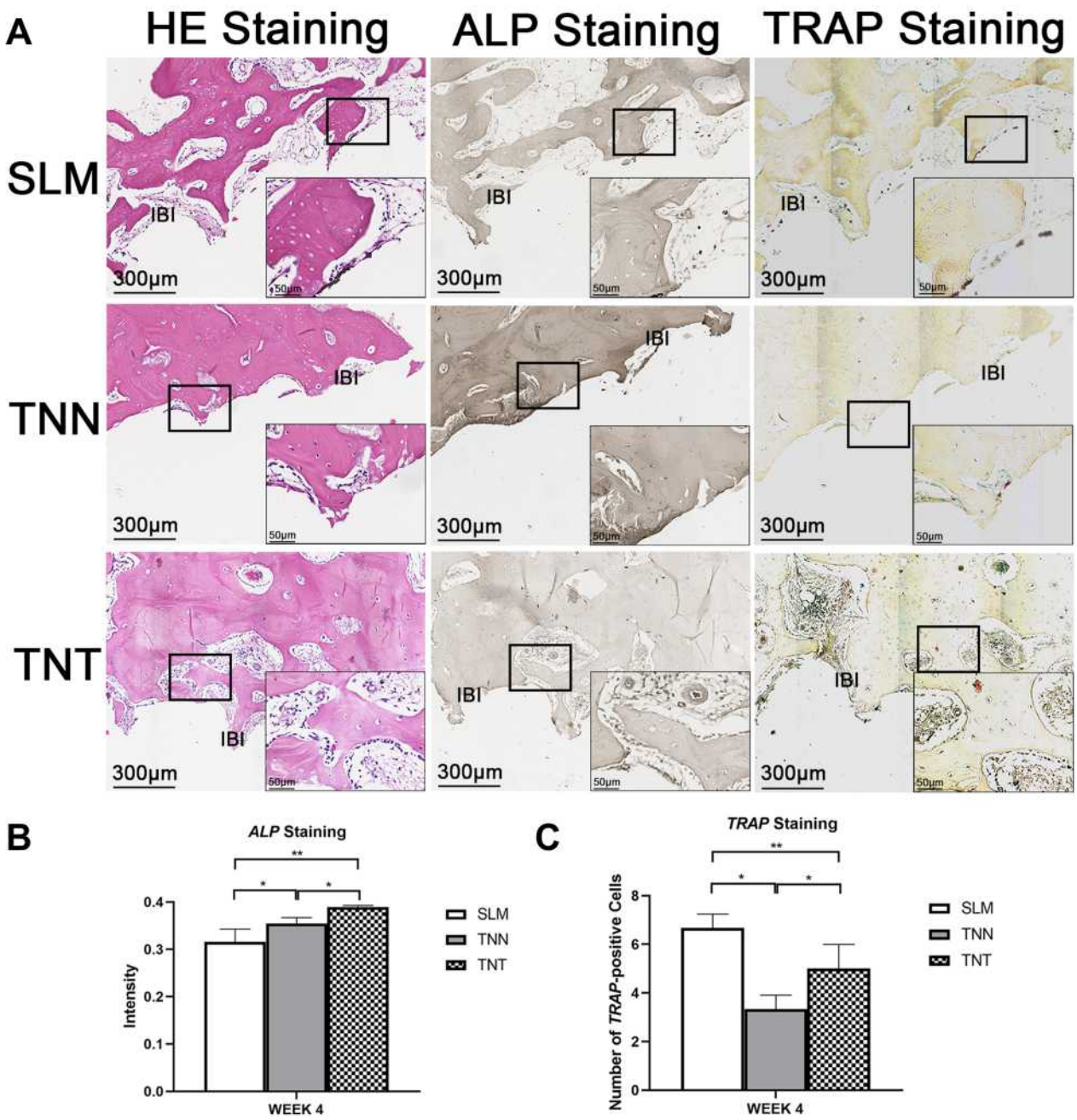

Figure 8 Histological analysis of paraffin sections: (**A**) HE staining, ALP staining and TRAP staining after 4 weeks (scale bar = 300 μm); (**B**) Statistical results of intensity in ALP staining; (**C**) Statistical results of TRAP positive cells count in TRAP staining. *P <0.05, **P <0.01.
Abbreviation: IBI, implant-bone interface.

Overall, on the one hand, TNTs exhibited superior osteogenesis promotion, on the other hand, TNNs showed stronger osteoclastogenesis inhibition *in vitro*. However, osteoblasts and osteoclasts interact each other in the remolding environment. Nagasawa et al. suggested that surface topography altered function of BMSC in order to influence BMM-derived osteoclastogenesis.[60] Lotz et al. demonstrated that surface treatments altered osteoblast lineage cells to regulate osteoclasts.[61] Therefore, we explored the *in vivo* process for further verification and obtained similar results. The BV/TV and BIC at week 4 were higher in TNT group than TNN group, while showing no difference at week 8. Taking the results of staining into consideration, TNT group can accelerate bone formation around implants in an early stage compared with TNN group, implying the

possibility for early loading of implants in clinical practice. By contrast, as the highest inhibition surface for osteoclast differentiation, TNN group might possibly prevent bone resorption and thus apply in diseases with inappropriate osteoclast activity such as osteoporosis and osteoarthritis.

Taken together, TNN and TNT groups both could promote osteogenesis and inhibit osteoclastogenesis at the same time, which are suitable as the substrates for further functionalization on SLM titanium. TNN had the stronger ability of inhibiting osteoclastogenesis while TNT promoted osteogenesis superiorly. These results would instruct us to choose appropriate SLM titanium substrate for further multifunctional surface modification for the sake of synergistic or complementary effects to achieve superior individualized application. However, limitations exist in this study and intercellular interactions between osteoblasts and osteoclasts influenced by topographies should be investigated in future studies.

Conclusion

In this study, TNN and TNT substrates of SLM titanium, the most commonly used substrates for multifunction, had proven dual advantages in promotion of osteogenesis and inhibition of osteoclastogenesis. Furthermore, TNN showed better capability in inhibiting osteoclast activity while TNT facilitated stronger osteogenesis. These results implied that TNT substrate would take advantage in early application after implantation, while diseases with excessive osteoclast activity would prefer TNN substrate. Therefore, our research would provide guidance when a biologically based first-step selection of combined-modifications needs to be made for different clinical purposes.

Acknowledgments

This work is funded by Guangdong Science and Technology Planning Project (No. 2019A050516001) and Foshan Science and Technology Innovation Project (No. 2018IT100212).

Disclosure

The authors report no conflicts of interest in this work.

References

1. Ligon SC, Liska R, Stampfl J, Gurr M, Mülhaupt R. Polymers for 3D printing and customized additive manufacturing. *Chem Rev*. 2017;117:10212–10290. doi:10.1021/acs.chemrev.7b00074
2. Zhu C, Pascall AJ, Dudukovic N, et al. Colloidal materials for 3D Printing. *Annu Rev Chem Biomol Eng*. 2019;10:17–42. doi:10.1146/annurev-chembioeng-060718-030133
3. Turnbull G, Clarke J, Picard F, et al. 3D bioactive composite scaffolds for bone tissue engineering. *Bioact Mater*. 2017;3:278–314. doi:10.1016/j.bioactmat.2017.10.001
4. Cai H, Liu Z, Wei F, Yu M, Xu N, Li Z. 3D printing in spine surgery. *Adv Exp Med Biol*. 2018;1093:345–359. doi:10.1007/978-981-13-1396-7_27
5. Shirazi SFS, Gharehkhani S, Mehrali M, et al. A review on powder-based additive manufacturing for tissue engineering: selective laser sintering and inkjet 3D printing. *Sci Technol Adv Mater*. 2015;16(3):033502. doi:10.1088/1468-6996/16/3/033502
6. Pattanayak DK, Fukuda A, Matsushita T, et al. Bioactive Ti metal analogous to human cancellous bone: fabrication by selective laser melting and chemical treatments. *Acta Biomater*. 2011;7:1398–1406. doi:10.1016/j.actbio.2010.09.034
7. Shaoki A, Xu JY, Sun H, et al. Osseointegration of three-dimensional designed titanium implants manufactured by selective laser melting. *Biofabrication*. 2016;8:045014. doi:10.1088/1758-5090/8/4/045014
8. Yan C, Hao L, Hussein A, Young P. Ti-6Al-4V triply periodic minimal surface structures for bone implants fabricated via selective laser melting. *J Mech Behav Biomed Mater*. 2015;51:61–73. doi:10.1016/j.jmbbm.2015.06.024
9. Tan XP, Tan YJ, Chow CSL, Tor SB, Yeong WY. Metallic powder-bed based 3D printing of cellular scaffolds for orthopaedic implants: a state-of-the-art review on manufacturing, topological design, mechanical properties and biocompatibility. *Mater Sci Eng C Mater Biol Appl*. 2017;76:1328–1343. doi:10.1016/j.msec.2017.02.094
10. Xu JY, Chen XS, Zhang CY, Liu Y, Wang J, Deng FL. Improved bioactivity of selective laser melting titanium: surface modification with micro-/nano-textured hierarchical topography and bone regeneration performance evaluation. *Mater Sci Eng C Mater Biol Appl*. 2016;68:229–240. doi:10.1016/j.msec.2016.05.096
11. Lee YH, Kim JS, Kim JE, et al. Nanoparticle mediated PPARγ gene delivery on dental implants improves osseointegration via mitochondrial biogenesis in diabetes mellitus rat model. *Nanomedicine*. 2017;13:1821–1832. doi:10.1016/j.nano.2017.02.020
12. Zhang W, Jin Y, Qian S, et al. Vacuum extraction enhances rhPDGF-BB immobilization on nanotubes to improve implant osseointegration in ovariectomized rats. *Nanomedicine*. 2014;10:1809–1818. doi:10.1016/j.nano.2014.07.002
13. Marycz K, Krzak-Roś J, Donesz-Sikorska A, Śmieszek A. The morphology, proliferation rate, and population doubling time factor of adipose-derived mesenchymal stem cells cultured on to non-aqueous SiO 2 TiO 2 and hybrid sol-gel-derived oxide coatings. *J Biomed Mater Res A*. 2014;102(11):4017–4026. doi:10.1002/jbm.a.35072
14. Boanini E, Torricelli P, Sima F, et al. Gradient coatings of strontium hydroxyapatite/zinc β-tricalcium phosphate as a tool to modulate osteoblast/osteoclast response. *J Inorg Biochem*. 2018;183:1–8. doi:10.1016/j.jinorgbio.2018.02.024
15. Braz JKFS, Martins GM, Morales N, et al. Live endothelial cells on plasma-nitrided and oxidized titanium: an approach for evaluating biocompatibility. *Mater Sci Eng C Mater Biol Appl*. 2020;113:111014. doi:10.1016/j.msec.2020.111014
16. Bosshardt DD, Chappuis V, Buser D. Osseointegration of titanium, titanium alloy and zirconia dental implants: current knowledge and open questions. *Periodontol 2000*. 2017;73:22–40. doi:10.1111/prd.12179
17. Albrektsson T, Dahlin C, Jemt T, Sennerby L, Turri A, Wennerberg A. Is marginal bone loss around oral implants the result of a provoked foreign body reaction? *Clin Implant Dent Relat Res*. 2014;16:155–165. doi:10.1111/cid.12142
18. Warnke PH, Douglas T, Wollny P, et al. Rapid prototyping: porous titanium alloy scaffolds produced by selective laser melting for bone tissue engineering. *Tissue Eng Part C Methods*. 2009;15:115–124. doi:10.1089/ten.tec.2008.0288

19. Tay CY, Irvine SA, Boey FY, Tan LP, Venkatraman S. Micro-/nano-engineered cellular responses for soft tissue engineering and biomedical applications. *Small*. 2011;7:1361–1378. doi:10.1002/smll.201100046
20. Wennerberg A, Albrektsson T. Effects of titanium surface topography on bone integration: a systematic review. *Clin Oral Implants Res*. 2009;20:172–184. doi:10.1111/j.1600-0501.2009.01775.x
21. Schwartz Z, Olivares-Navarrete R, Wieland M, Cochran DL, Boyan BD. Mechanisms regulating increased production of osteoprotegerin by osteoblasts cultured on microstructured titanium surfaces. *Biomaterials*. 2009;30:3390–3396. doi:10.1016/j.biomaterials.2009.03.047
22. Park JW, Han SH, Hanawa T. Effects of surface nanotopography and calcium chemistry of titanium bone implants on early blood platelet and macrophage cell function. *Biomed Res Int*. 2018;2018:1362958. doi:10.1155/2018/1362958
23. Xu R, Hu X, Yu X, et al. Micro-/nano-topography of selective laser melting titanium enhances adhesion and proliferation and regulates adhesion-related gene expressions of human gingival fibroblasts and human gingival epithelial cells. *Int J Nanomedicine*. 2018;13:5045–5057. doi:10.2147/IJN.S166661
24. Mendonça G, Mendonça DB, Aragão FJ, Cooper LF. Advancing dental implant surface technology–from micron- to nanotopography. *Biomaterials*. 2008;29:3822–3835. doi:10.1016/j.biomaterials.2008.05.012
25. Huo K, Gao B, Fu J, Zhao L, Chu PK. Fabrication, modification, and biomedical applications of anodized TiO_2 nanotube arrays. *RSC Adv*. 2014;4:17300–17324. doi:10.1039/C4RA01458H
26. Cheng Y, Yang H, Yang Y, et al. Progress in TiO_2 nanotube coatings for biomedical applications: a review. *J Mater Chem B*. 2018;6:1862–1886. doi:10.1039/c8tb00149a
27. Cheng H, Xiong W, Fang Z, et al. Strontium (Sr) and silver (Ag) loaded nanotubular structures with combined osteoinductive and antimicrobial activities. *Acta Biomater*. 2016;31:388–400. doi:10.1016/j.actbio.2015.11.046
28. Liu X, Zhang Y, Li S, et al. Study of a new bone-targeting titanium implant-bone interface. *Int J Nanomedicine*. 2016;11:6307–6324. doi:10.2147/IJN.S119520
29. Abrams GA, Goodman SL, Nealey PF, Franco M, Murphy CJ. Nanoscale topography of the basement membrane underlying the corneal epithelium of the rhesus macaque. *Cell Tissue Res*. 2000;299:39–46. doi:10.1007/s004419900074
30. Kato E, Sakurai K, Yamada M. Periodontal-like gingival connective tissue attachment on titanium surface with nano-ordered spikes and pores created by alkali-heat treatment. *Dent Mater*. 2015;31:e116–130. doi:10.1016/j.dental.2015.01.014
31. Nishiguchi S, Kato H, Fujita H, et al. Titanium metals form direct bonding to bone after alkali and heat treatments. *Biomaterials*. 2001;22:2525–2533. doi:10.1016/s0142-9612(00)00443-9
32. Kim HM, Miyaji F, Kokubo T, Nakamura T. Preparation of bioactive Ti and its alloys via simple chemical surface treatment. *J Biomed Mater Res*. 1996;32:409–417. doi:10.1002/(SICI)1097-4636(199611)32:3<409::AID-JBM14>3.0.CO;2-B
33. Miyaza T, Kim HM, Kokubo T, Ohtsuki C, Kato H, Nakamura T. Mechanism of bonelike apatite formation on bioactive tantalum metal in a simulated body fluid. *Biomaterials*. 2002;23:827–832. doi:10.1016/s0142-9612(01)00188-0
34. Muramatsu K, Uchida M, Kim HM, Fujisawa A, Kokubo T. Thromboresistance of alkali- and heat-treated titanium metal formed with apatite. *J Biomed Mater Res A*. 2003;65:409–416. doi:10.1002/jbm.a.10494
35. Zhao CY, Zhu XD, Yuan T, Fan HS, Zhang XD. Fabrication of biomimetic apatite coating on porous titanium and their osteointegration in femurs of dogs. *Mater Sci Eng C Mater Biol Appl*. 2010;30:98–104. doi:10.1016/j.msec.2009.09.004
36. Li P, Ducheyne P. Quasi-biological apatite film induced by titanium in a simulated body fluid. *J Biomed Mater Res*. 1998;41:341–348. doi:10.1002/(sici)1097-4636(19980905)41:3<341::aid-jbm1>3.0.co;2-c
37. Alvarez K, Nakajima H. Metallic scaffolds for bone regeneration. *Materials*. 2009;2:790–832. doi:10.3390/ma2030790
38. Wang H, Xu Q, Hu H, et al. The fabrication and function of strontium-modified hierarchical micro/nano titanium implant. *Int J Nanomedicine*. 2020;15:8983–8998. doi:10.2147/IJN.S268657
39. Huang J, Zhang X, Yan W, et al. Nanotubular topography enhances the bioactivity of titanium implants. *Nanomedicine*. 2017;13:1913–1923. doi:10.1016/j.nano.2017.03.017
40. Su Y, Komasa S, Sekino T, Nishizaki H, Okazaki J. Nanostructured Ti6Al4V alloy fabricated using modified alkali-heat treatment: characterization and cell adhesion. *Mater Sci Eng C Mater Biol Appl*. 2016;59:617–623. doi:10.1016/j.msec.2015.10.077
41. Kylmaoja E, Nakamura M, Tuukkanen J. Osteoclasts and remodeling based bone formation. *Curr Stem Cell Res Ther*. 2016;11:626–633. doi:10.2174/1574888x10666151019115724
42. Pan C, Hu Y, Gong Z, et al. Improved blood compatibility and endothelialization of titanium oxide nanotube arrays on titanium surface by zinc doping. *ACS Biomater Sci Eng*. 2020;6:2072–2083. doi:10.1021/acsbiomaterials.0c00187
43. Wu Y, Tang H, Liu L, et al. Biomimetic titanium implant coated with extracellular matrix enhances and accelerates osteogenesis. *Nanomedicine (Lond)*. 2020;15:1779–1793. doi:10.2217/nnm-2020-0047
44. Yang Z, Xi Y, Bai J, et al. Covalent grafting of hyperbranched poly-L-lysine on Ti-based implants achieves dual functions of antibacteria and promoted osteointegration in vivo. *Biomaterials*. 2020;16:120534. doi:10.1016/j.biomaterials.2020.120534
45. Shen X, Zhang Y, Ma P, et al. Fabrication of magnesium/zinc-metal organic framework on titanium implants to inhibit bacterial infection and promote bone regeneration. *Biomaterials*. 2019;212:1–16. doi:10.1016/j.biomaterials.2019.05.008
46. Li G, Cao H, Zhang W, et al. Enhanced osseointegration of hierarchical micro/nanotopographic titanium fabricated by microarc oxidation and electrochemical treatment. *ACS Appl Mater Interfaces*. 2016;8:3840–3852. doi:10.1021/acsami.5b10633
47. Tsukanaka M, Fujibayashi S, Takemoto M, et al. Bioactive treatment promotes osteoblast differentiation on titanium materials fabricated by selective laser melting technology. *Dent Mater J*. 2016;35:118–125. doi:10.4012/dmj.2015-127
48. Zhang Y, Chen SE, Shao J, van den Beucken JJJP. Combinatorial surface roughness effects on osteoclastogenesis and osteogenesis. *ACS Appl Mater Interfaces*. 2018;10:36652–36663. doi:10.1021/acsami.8b10992
49. Zhou Y, Wang YB, Zhang EW, et al. Alkali-heat treatment of a low modulus biomedical Ti-27Nb alloy. *Biomed Mater*. 2009;4:044108. doi:10.1088/1748-6041/4/4/044108
50. Albrektsson T, Wennerberg A. On osseointegration in relation to implant surfaces. *Clin Implant Dent Relat Res*. 2019;21:4–7. doi:10.1111/cid.12742
51. Wang N, Li H, Lü W, et al. Effects of TiO_2 nanotubes with different diameters on gene expression and osseointegration of implants in minipigs. *Biomaterials*. 2011;32:6900–6911. doi:10.1016/j.biomaterials.2011.06.023
52. Gersbach CA, Le Doux JM, Guldberg RE, García AJ. Inducible regulation of Runx2-stimulated osteogenesis. *Gene Ther*. 2006;13:873–882. doi:10.1038/sj.gt.3302725
53. Otto F, Thornell AP, Crompton T, et al. Cbfa1, a candidate gene for cleidocranial dysplasia syndrome, is essential for osteoblast differentiation and bone development. *Cell*. 1997;89:765–771. doi:10.1016/s0092-8674(00)80259-7
54. Manrique N, Pereira CC, Luvizuto ER, et al. Hypertension modifies OPG, RANK, and RANKL expression during the dental socket bone healing process in spontaneously hypertensive rats. *Clin Oral Investig*. 2015;19:1319–1327. doi:10.1007/s00784-014-1369-0
55. Stan MS, Memet I, Fratila C, Krasicka-Cydzik E, Roman I, Dinischiotu A. Effects of titanium-based nanotube films on osteoblast behavior in vitro. *J Biomed Mater Res A*. 2015;103:48–56. doi:10.1002/jbm.a.35148

56. Otero JE, Dai S, Alhawagri MA, Darwech I, Abu-Amer Y. IKKbeta activation is sufficient for RANK-independent osteoclast differentiation and osteolysis. *J Bone Miner Res*. 2010;25:1282–1294. doi:10.1002/jbmr.4
57. Asagiri M, Sato K, Usami T, et al. Autoamplification of NFATc1 expression determines its essential role in bone homeostasis. *J Exp Med*. 2005;202:1261–1269. doi:10.1084/jem.20051150
58. Yamashita T, Yao Z, Li F, et al. NF-kappaB p50 and p52 regulate receptor activator of NF-kappaB ligand (RANKL) and tumor necrosis factor-induced osteoclast precursor differentiation by activating c-Fos and NFATc1. *J Biol Chem*. 2007;282:18245–18253. doi:10.1074/jbc.M610701200
59. Yang J, Yu X, Zhang Z, et al. Surface modification of titanium manufactured through selective laser melting inhibited osteoclast differentiation through mitogen-activated protein kinase signaling pathway. *J Biomater Appl*. 2020;35:169–181. doi:10.1177/0885328220920457
60. Nagasawa M, Cooper LF, Ogino Y, et al. Topography influences adherent cell regulation of osteoclastogenesis. *J Dent Res*. 2016;95:319–326. doi:10.1177/0022034515616760
61. Lotz EM, Berger MB, Schwartz Z, Boyan BD. Regulation of osteoclasts by osteoblast lineage cells depends on titanium implant surface properties. *Acta Biomater*. 2018;68:296–307. doi:10.1016/j.actbio.2017.12.039